

Type of the Paper (Article, Review, Communication, etc.)

Rainfall prediction with AMSR-E soil moisture products using SM2RAIN and nonlinear autoregressive networks with exogenous input (NARX) for poorly gauged basins: Application to the Karkheh river basin, Iran

Majid Fereidoon ^{1,*} and Manfred Koch ¹

¹ Department of Geotechnology and Geohydraulics, University of Kassel, 34125 Kassel, Germany; majid.fereidoon@gmail.com

* Correspondence: majid.fereidoon@gmail.com; Tel.: +49 561 804 3408

Abstract: Accurate estimates of daily rainfall are essential for understanding and modeling the physical processes involved in the interaction between the land surface and the atmosphere. In this study, daily satellite soil moisture observations from the Advanced Microwave Scanning Radiometer - Earth Observing System (AMSR-E) generated by implementing the standard NASA-algorithm are employed for estimating rainfall, firstly, through the use of recently developed approach, SM2RAIN (Brocca et al., 2013) and, secondly, the nonlinear autoregressive network with exogenous inputs (NARX) neural modelling at five climate stations in the Karkheh river basin (KRB), located in southwest Iran. In the SM2RAIN method, the period 1 January 2003 to 31 December 2005 is used for the calibration of algorithm and the remaining 9 months from 1 January 2006 to 30 September 2006 is used for the validation of the rainfall estimates. In the NARX model, the full study period is split into a training (1 January 2003 to 31 September 2005) and a testing (1 September 2005 to 30 September 2006) stage. For the prediction of the rainfall as the desired target (output), relative soil moisture changes from AMSR-E and measured air temperature time series are chosen as exogenous (external) inputs in NARX. The quality of the estimated rainfall data is evaluated by comparing it with observed rainfall data at the five rain gauges in terms of the correlation coefficient R, the RMSE and the statistical bias. For the SM2RAIN method, R ranges between 0.44 and 0.9 for all stations, whereas for the NARX- model the values are generally slightly lower. Moreover, the values of the bias for each station indicate that although SM2RAIN is likely to underestimate large rainfall intensities, due to the known effect of soil moisture saturation, its biases are somewhat lower than those of NARX. In conclusion, the results of the present study show that with the use of AMSR-E soil moisture products in the physically based SM2RAIN- algorithm as well as in the NARX neural network, rainfall for poorly gauged regions can be fairly predicted.

Keywords: Soil moisture; NARX neural networks; AMSR-E; SM2RAIN; Karkheh River Basin

1. Introduction

Rainfall as a natural phenomenon plays an important role in driving the hydrological cycle. Precise information on the amount and distribution of rainfall is indispensable in many hydrological applications, e.g. climate change assessment, drought monitoring, flood forecasting and extreme weather prediction [1-3].

Rain gauges and satellite rainfall products are two most widely used sources of data for rainfall measurements [4]. Although individual rain gauges provide rainfall values at relatively high

accuracy, their often sparse regional coverage limits the spatial resolution of rainfall measurements required for the kind of hydrological studies mentioned above. Difficulties in estimating rainfall have been addressed in many studies [5,6], especially in developing countries where ground-based rainfall networks may be sparse or even nonexistent [7]. In fact, areal rainfall data from even a dense rain gauge network may be highly uncertain [8,9], as the spatial distribution of rainfall is usually obtained by some kind of geostatistical interpolation of point rainfall data (e.g. [10-14]).

Another alternative approach for proper rainfall estimation is offered by satellite rainfall products [15,17]. The recent satellite-based rainfall products can provide accurate rainfall data sets at high spatial and temporal resolutions for a wide range of hydrological applications [18,19]. [20] presented a preliminary analysis of the potential for using satellite rainfall estimates through a comparison with available point gauge data for four poorly gauged river basins in South Africa, Zambia, and Angola.

A large number of satellite rainfall products with steadily increasing spatial and temporal resolution have become available since the 1990s, e.g. Precipitation Estimation from Remotely Sensed Information using Artificial Neural Networks (PERSIANN) [21,22]; The Tropical Rainfall Measuring Mission (TRMM), and the PMW-calibrated IR algorithm (PMIR) [23]. [24] first assessed the performance of four latest and widely used satellite-based precipitation datasets, namely CMORPH CRT, CMORPH BLD, PERSIANN CDR, TMPA 3B42 version 7 over the upper Yellow river basin in China during the 2001–2012 time period for the simulation of streamflow for two flood events. Whereas the 2005-flood event was well predicted for all four satellite-based precipitation data sets, they did poorly for the 2012- flood event, as the latter was induced by more torrential rainfall with larger estimation errors.

Another way to estimate rainfall time series is to build a prediction model with satellite surface soil moisture products. A novel approach named SM2RAIN proposed by [25] employs soil moisture observations to infer the rainfall. This technique is based on the inversion of water balance equation and has already been successfully applied to in-situ [25] and satellite soil moisture data [26-29] in different regions. [30] employed the obtained rainfall estimates through SM2RAIN in hydrological modeling to predict the river discharge over four catchments in Italy during the 4-year period 2010–2013. [31] used SM2RAIN- corrected daily rain gauge data in flood modeling in a small watershed in southern France and showed the superiority of this correction approach over the use of rain gauge data alone.

As calibration and validation of SM2RAIN model for estimating water balance components and rainfall constitutes a time-consuming iterative process, other non-parametric approaches such as artificial neural networks (ANNs) have been proposed and applied to the prediction of complex physical systems, such as rainfall, in many parts of the world (e.g. [32-36]). However, in most of these studies ANN has been used in the form of a classical input-output multi-perceptron model between various climate components as input and rainfall as output, with only a few taking into account likely (auto) lagged relationships in the climate variables and/or the rainfall [37].

This deficiency of classical ANN in describing time-lagged input-output correlations is partly remedied by the NARX (Nonlinear Auto-Regressive with Exogenous Inputs) neural network model introduced by [38] as a new representation for a wide range of discrete and nonlinear systems. NARX is a dynamic neural network that uses time delays as well as feedback (memory) connections between both output and input layers to come up with more reliable ANN-prediction models [39,40].

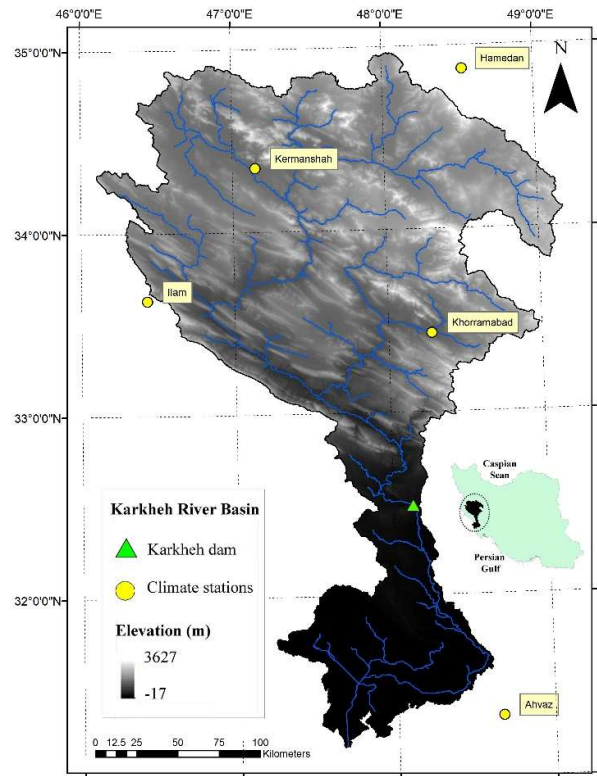
[41] applied NARX successfully to obtain groundwater level forecasts for several wells in three different types of aquifers, namely porous, fractured and karst aquifers in southwest Germany, using precipitation and temperature as input parameters.

In this paper we describe a new application of the NARX neural network to better predict continuous rainfall series across the Karkheh river basin (KRB), Iran, which has been the focus of several studies of the authors over the last years (e.g. [42]). To this avail, changes of relative AMSR-E satellite soil moisture and measured temperature data are considered as input data in NARX to estimate the rainfall. These estimates are then compared with the ground-based observations as well as with those obtained by [29] using the SM2RAIN approach.

95 2. Materials and Methods

96 2.1. Study area and ground based data collection

97 The study area, Karkheh river basin (KRB), is located in southwest Iran between 30°58–34°56 N
98 latitude and 46°06–49°10 E longitude (Figure 1). KRB is about 51,000 km2 in size and contains a
99 relatively flat topography (i.e. < 100 m) in its southern- and mountainous areas of the Zagros of up to
100 3600 MASL in the northern parts.
101



102
103 **Figure 1.** Map of the Karkheh river basin with weather stations and the Karkheh dam

104 The climate of the basin is mainly characterized by Mediterranean climate conditions with
105 annual rainfall varying from 150 to 250 mm in the flat south and from 550 to 750 mm in the
106 mountainous north [42,43].

107 **Table 1.** Geographical characteristics of the selected climate stations

Climate Station	Longitude (degrees East)	Latitude (degrees North)	Elevation (masl)
Hamedan	48.53	34.87	1741
Kermanshah	47.15	34.35	1319
Ilam	46.43	33.63	1337
Khorramabad	48.28	33.43	1148
Ahvaz	48.67	31.33	22

108
109 In the middle and upper reaches, the coldest month of the year, January, experiences a mean
110 temperature of -2 °C, and the warmest month, August, of 29 °C. In the lower regions of the KRB, the
111 annual mean temperature fluctuates from 3°C to 9°C during wintertime and 36°C to 41°C in
112 summertime [44].

Climatological data for daily precipitation, maximum and minimum air temperature from 5 weather stations (Table 1) for the time period January 2003 - October 2006 – the time interval with the less number of gaps for all stations - are obtained from Iran Meteorology Department.

2.2. AMSR-E soil moisture product data

The Advanced Microwave Scanning Radiometer (AMSR-E) on board of NASA's Aqua satellite was a passive microwave radiometer observing brightness temperatures at six different frequencies, ranging from 6.9 to 89.0 GHz since May 2002, with daily ascending (13:30 equatorial local crossing time) and descending (01:30 equatorial local crossing time) overpasses, over a swath width of 1445 km. It stopped producing data in October 2011 after more than 9 years observation, due to some technical problems with the antenna. Several algorithms are applied to retrieve soil moisture products from AMSR-E. In this study, the daily soil moisture data based on NASA algorithm [45,46] are derived directly from gridded Level-3 land surface product (AE_Land3) for the same time period as for the ground-based climate data above (January 2003 - October 2006).

2.3. AMSR-E soil moisture product data

Based on the land phase of hydrological cycle, the spatial distribution of rainfall $p(t)$ across a watershed at each time step is calculated from the classical, rearranged water balance equation:

$$p(t) = nZ ds(t)/dt + q(t) + e(t) + g(t) \quad (1)$$

where $n[-]$ is the soil porosity, $Z[L]$ is the soil layer depth, $s(t)[-]$ is the relative soil moisture, $t[T]$ is the time and p , q , e and $g[L/T]$ are the precipitation, surface runoff, evapotranspiration, and drainage rate, respectively. By solving this equation and knowing all other components of the hydrological cycle, the rainfall for each time step can be estimated from soil moisture data [25,26]. It should be noted that and as shown by [47], the surface runoff q can assumed to be negligible.

$$g(t) = a s(t)^b \quad (2)$$

The drainage rate $g(t)$ is estimated with the following equation [48]. The actual evapotranspiration rate $e(t)$ is represented by a product of the potential evapotranspiration $ET_p(t)$ and the relative soil moisture $s(t)$ (e.g., [27]):

$$e(t) = ET_p(t) \times s(t) \quad (3)$$

where $ET_p(t)$ is calculated by means of the theoretical Blaney and Criddle approach as modified by [51]:

$$ET_p(t) = -2 + c[\xi(0.46T_a(t) + 8.13)] \quad (4)$$

where $T_a[^\circ\text{C}]$ is the mean air temperature, ξ is the fraction of daytime hours for the time step used (daily time step in this study) in the total daytime hours of the year, and c is a parameter - to be determined in the calibration process further down - that depends on the daytime wind speed, minimum relative humidity and actual insolation time. Although a value of $c=1.26$ has been proposed for this parameter in many studies (see e.g., [49]), it will be further optimized in the calibration/validation process within an acceptable range (0.8-2.1). The parameter values in equations 2-4 (nZ , a , b , and c) are calibrated for reproducing observed rainfall data.

2.4. AMSR-E soil moisture product data

2.4.1. ANN-basics and classification

An Artificial Neural Network (ANN) is a computational approach that has been widely used since the 1990's in various fields of science, involving function estimation, time series forecasting (e.g. [50]) and classification purposes ([51]). The major advantage of using an ANN model instead of deterministic modeling is that the former allows the determination of complicated nonlinear function relationships between some input (action) variables and output (reaction) variables for which the physics is not known a priori. For further details on the concepts and methodology of ANN the reader is referred to the still! seminal book of [52]. Neural networks can be categorized as either static or dynamic. In a static (feedforward) network the information moves in only one direction from the input to the output (target), irrespective of time, so that there is no feedback from (previous) values of the input and/or output signal. In contrast, in a dynamic network [53] output (target) depends on values of the input and/or output at previous times, i.e. reflecting some kind of inherent memory in the series, as it is prevalent in many scientific fields, namely hydrology and meteorology [54] and often described by some autocorrelation. More specifically, dynamic neural networks can then be further divided into time-delay networks (output depends on previous values of input) and feedback (recurrent) (output depends on previous values of output) networks [55,56]. Dynamic neural networks are particularly suitable for nonlinear dynamic systems modeling and have been used in many applications involving time series modeling and prediction.

2.4.2. Nonlinear autoregressive neural network with exogenous inputs (NARX)

The nonlinear autoregressive network with exogenous inputs (NARX) is an important class of a dynamic network which encompasses the two features above, i.e. a time-delayed nonlinear input (x) - output (y) relationship (NX) and the auto-regressive properties of the output Y (AR) [39,56,57]. The general input-output formulation of a NARX model is as follows:

$$y(t) = f(y(t-1), y(t-2), \dots, y(t-d), x(t-1), x(t-2), \dots, x(t-d)) + \epsilon(t), \quad (5)$$

i.e. predicted values of the dependent variable $y(t)$ at time t is regressed on given d past values of series y and up to d previous values of an independent (exogenous) input signal $x(t)$.

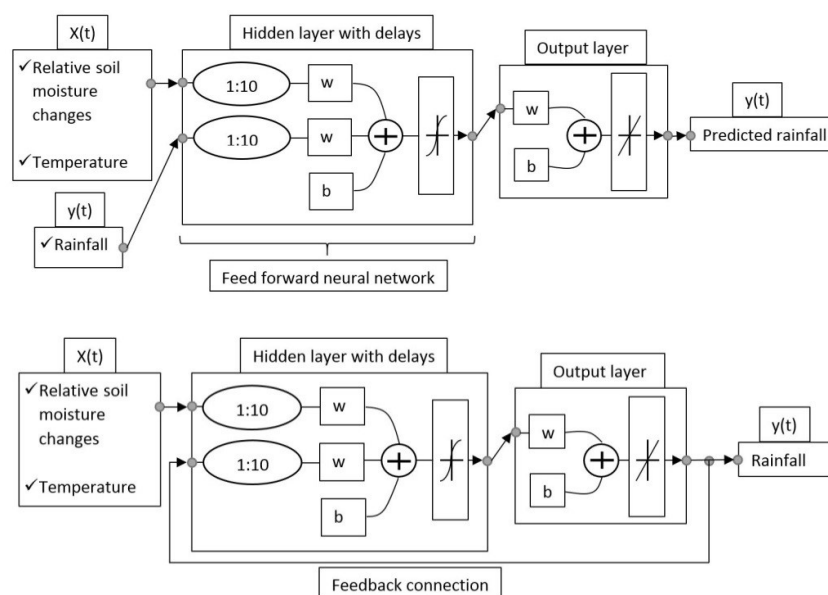


Figure 2. Recurrent neural model (NARX network in open-loop (upper panel) and closed-loop (lower panel) architecture according to Beale et al., 2012, with an example of $d=10$ delays).

The process of the NARX- network training is usually performed in open-loop form, using known historical values of the input x , i.e. relative soil moisture changes and air temperatures, and output y , i.e. rainfall (see Figure 2, upper panel) and in closed-loop form for subsequent

180 multistep-ahead prediction of y (see Figure 2, lower panel). In order to obtain an accurate
181 prediction model, speed up the calculation and to avoid overfitting, it is important to adjust the
182 maximum number of delays d in Eq. 5. Both the SM2RAIN- and the NARX neural network are
183 implemented within the MATLAB® - environment [58].

184 **3. Results and discussions**

185 As mentioned in the introduction, two different approaches of daily rainfall estimation in the
186 KRB, i.e. (1) the SM2RAIN algorithm incorporating soil moisture observations from AMSR-E and (2)
187 the NARX neural network algorithm also employing AMSR-E soil moisture observations and
188 ground-based mean air temperature as input and gauge-measured rainfall as output are used and
189 compared to each other.

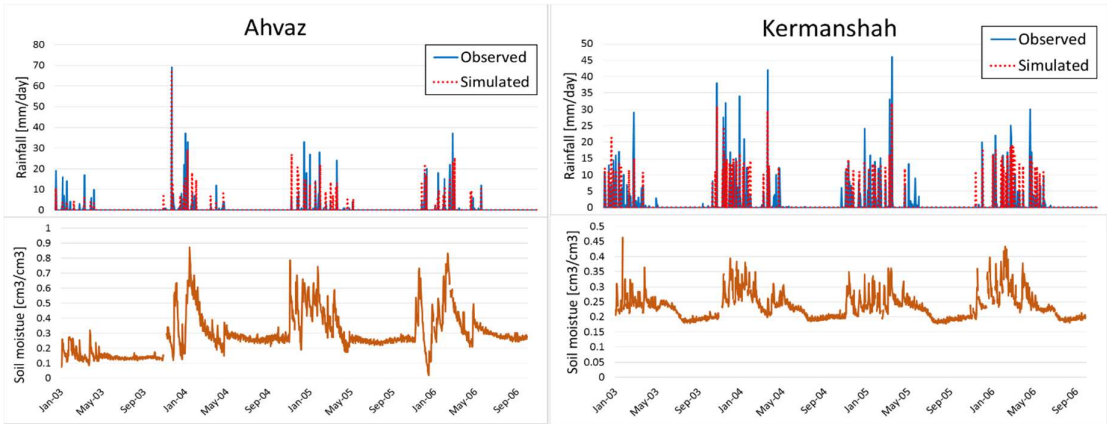
190 *3.1. SM2RAIN- rainfall estimation using AMSR-E soil moisture data*

191 The SM2RAIN model is calibrated using AMSRE soil moisture and gauge rainfall data for the
192 period 1 January 2003 to 31 December 2005 and validated with data for the remaining 9 months from
193 1 January 2006 to 30 September 2006. The calibration is performed as an iterative process wherefore
194 the free parameters in the SM2RAIN algorithm (Equations 1-4) are adjusted within their allowable
195 ranges, until the estimated rainfall values are in line with the measured ones, using the correlation
196 coefficient (R) and the root-mean-square error (RMSE) as quantitative statistical measures.

197 Time series of the daily SM2R-AMSRE- estimated and observed rainfall for the different stations
198 are shown in the upper panels of Figure 3, with the AMSR-E soil moisture time series depicted in the
199 corresponding lower panels. Table 2 lists the R and RMSE values of the SM2RAIN model fits obtained
200 for the 5 KRB climate stations for both the calibration and validation periods. One may notice from
201 the table that the observed rainfall data are reproduced with reasonable accuracy. In the validation
202 period, the R -values range between 0.57 for Khorramabad to 0.90 for Ilam. The RMSE is the lowest
203 for Ahvaz station, in accordance with the better R -value there. Lower performances are acquired for
204 Ilam and Khorramabad stations, most likely due to the presence of more noise in the associated
205 satellite soil moisture data (see Figure 3).

206

207



208

209

210
211

212
213
214
215
216
217
218

219
220

221
222
223
224
225

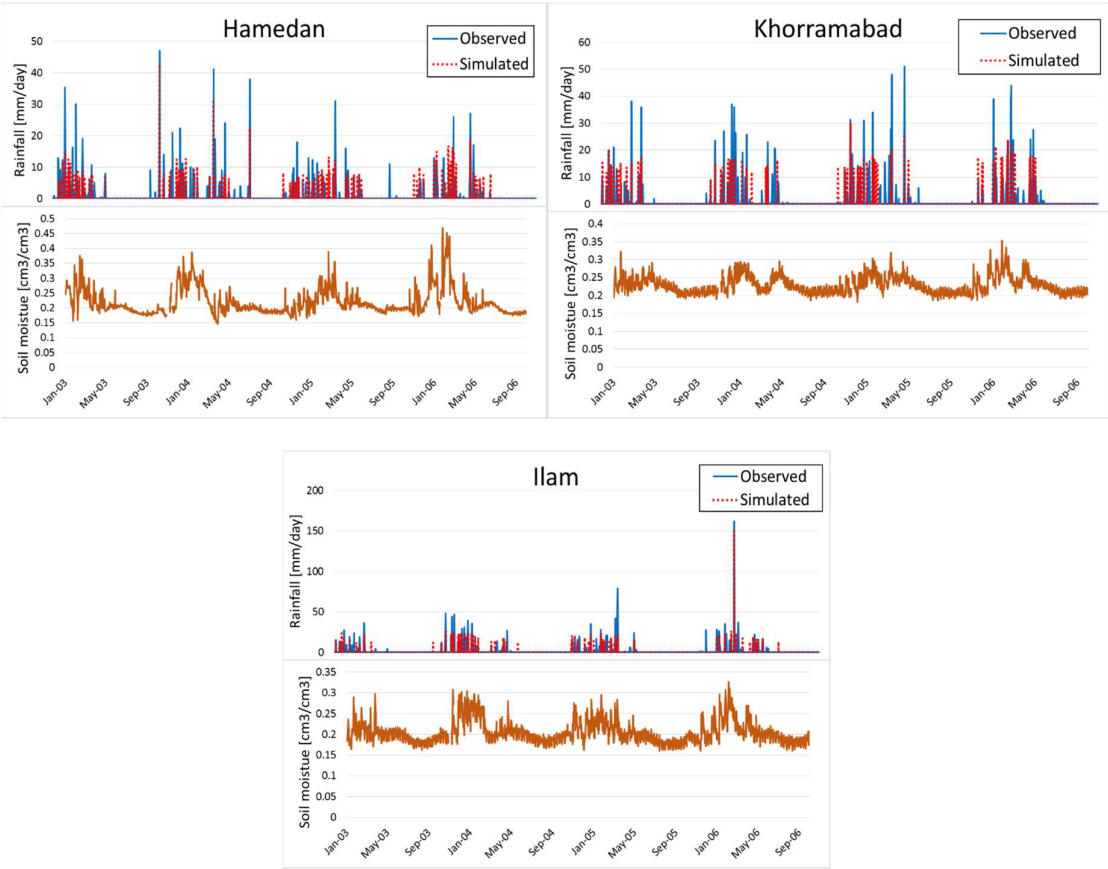


Figure 3. Observed and SM2RAIN-estimated rainfall (upper panels) and original AMSR-E soil moisture data (lower panels) from January 2003 to October 2006.

Besides, surface conditions and topography of the climate stations affect the outcome as well. Thus, the high altitude stations Ilam and Khorramabad stations in the mountainous regions, with more snow cover and frozen soils, do worse than the low altitude station Ahvaz.

Comparisons between the gauge-measured and SM2R-AMSRE estimated rainfall show that the SM2RAIN underestimates the total rainfall amount at all sites. The major reason for this are the constant values of soil moisture for any rainfall amount after reaching saturation [25,47,59,60].

Table 2. Correlation coefficient (R) and root-mean-square error (RMSE) of SM2RAIN- model fit of rainfall at the 5 KRB climate stations for calibration and validation periods

Climate Station	R [-]		RMSE [mm]	
	Cal	Val	Cal	Val
Ahvaz	0.75	0.66	2.5	2.5
Kermanshah	0.69	0.47	3.07	3.91
Hamedan	0.61	0.54	3.06	0.12
Khorramabad	0.57	0.57	4.19	4.32
Ilam	0.44	0.90	5.58	4.47

The optimized values of the four parameters (after calibration/validation) that control the water cycle in SM2RAIN method (see Equations 1-3) are listed in Table 3. Similar to [25,47], the values of these parameters are consistent with their expected physical ones.

Table 3. Optimized parameter values of the SM2RAIN-equations (1-3) for the 5 KRB climate stations.

Climate Station	Zn [mm]	a [mm/day]	b	c
Ahvaz	32.1	39	2.2	1.90
Kermanshah	34.8	50	2.3	2.00
Hamedan	58.3	56	1.5	1.20
Khorramabad	39.2	46	1.9	1.95
Ilam	44.6	87	2.5	1.90

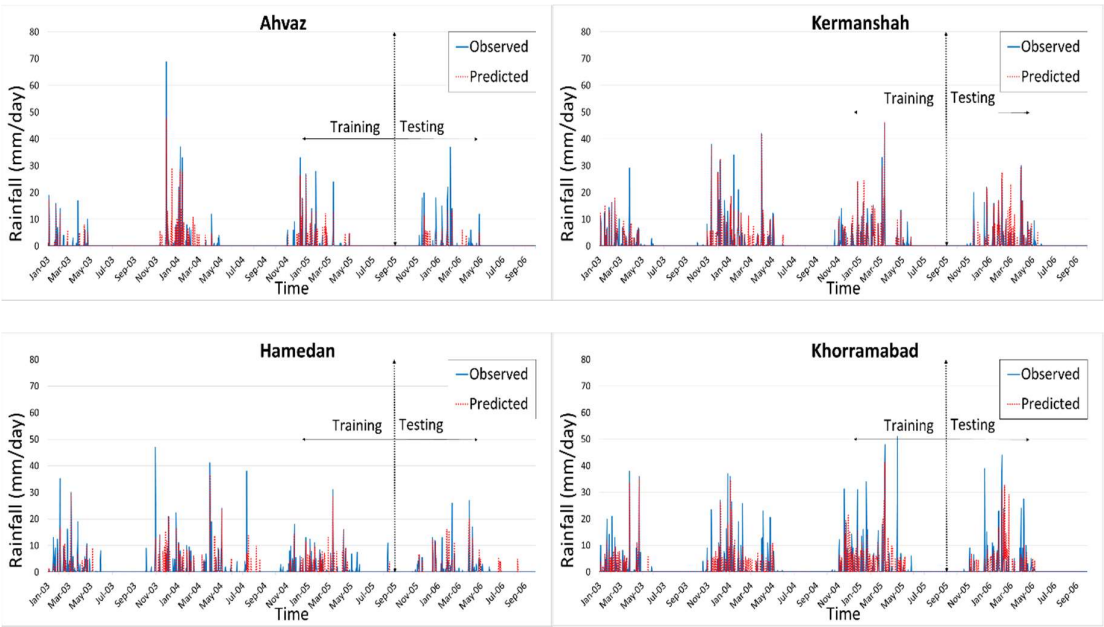
3.2. Rainfall estimation using the NARX neural network

Using AMSRE- satellite data for soil moisture, ground-measured temperatures and rainfall as input (open-loop, see Figure 2) and output, the new NARX- neural forecasting model was trained iteratively for the time period January 2003 to September 2005, by adjusting the number of hidden neurons and delays for each KRB-station, until a minimal RMSE was obtained. The subsequent testing was performed in closed-loop setup with data in the period September 2005 to September 2006. As mentioned, the application of the NARX-model requires the tuning of several parameters of the neural network. Table 4 presents the optimal number of hidden neurons and delays d (Equation 5) found after some lengthy trial-and-error runs to get the best results in terms of the least RMSE.

Table 4. Optimal number of hidden neurons and delays d for the NARX-model at 5 KRB stations

Climate Station	Neurons	Delays
Ahvaz	8	10
Kermanshah	10	8
Hamedan	9	10
Khorramabad	14	10
Ilam	10	12

Using the parameters of Table 4, Figure 4 shows the average NARX- estimated daily rainfall for the training and testing periods for the 5 KRB stations.



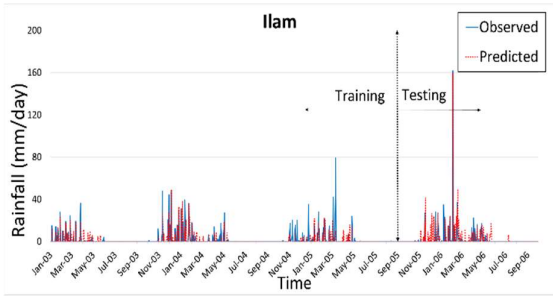


Figure 4. Observed and NARX- model- predicted daily rainfall for the KRB stations for training and testing stages

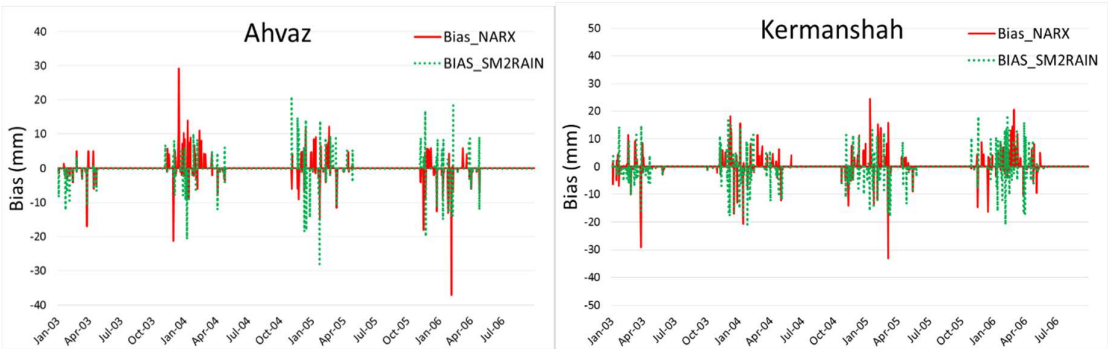
Furthermore, the training and one-year prediction accuracies of the NARX model were evaluated by the correlation coefficient (R) and the root-mean-square error (RMSE), both of which are listed in Table 5. Similar to the results of the SM2RAIN method in the previous section, the best and worst NARX model performances are obtained for stations Ahvaz and Khorramabad, respectively, with R-values ranging between 0.77 for the former and 0.44 for latter in the testing phase.

Table 5. Correlation coefficient (R) and root-mean-square error (RMSE) of the NARX-model fits for the 5 KRB climate stations for the training and testing phases

Climate Station	R [-]		RMSE [mm]	
	R [-]	RMSE [mm]	R [-]	RMSE [mm]
Ahvaz	0.81	3.3	0.76	4.8
Kermanshah	0.78	4.8	0.61	6.6
Hamedan	0.64	5.8	0.51	6.8
Khorramabad	0.61	5.9	0.42	7.3
Ilam	0.57	6.3	0.48	8.9

3.3. Comparison of SM2RAIN- and NARX- simulated rainfall

Comparison of the rainfall series predicted by NARX (Figure 4) with those of SM2RAIN (Figure 3) as well as of the corresponding statistical performance indicators (Tables 5 and 3) shows that for climate stations Ahvaz and Kermanshah the simulated NARX-predicted rainfall has a higher correlation with the observed one than the SM2RAIN-predicted one, and this holds for both training/calibration and testing/validation phases/periods.



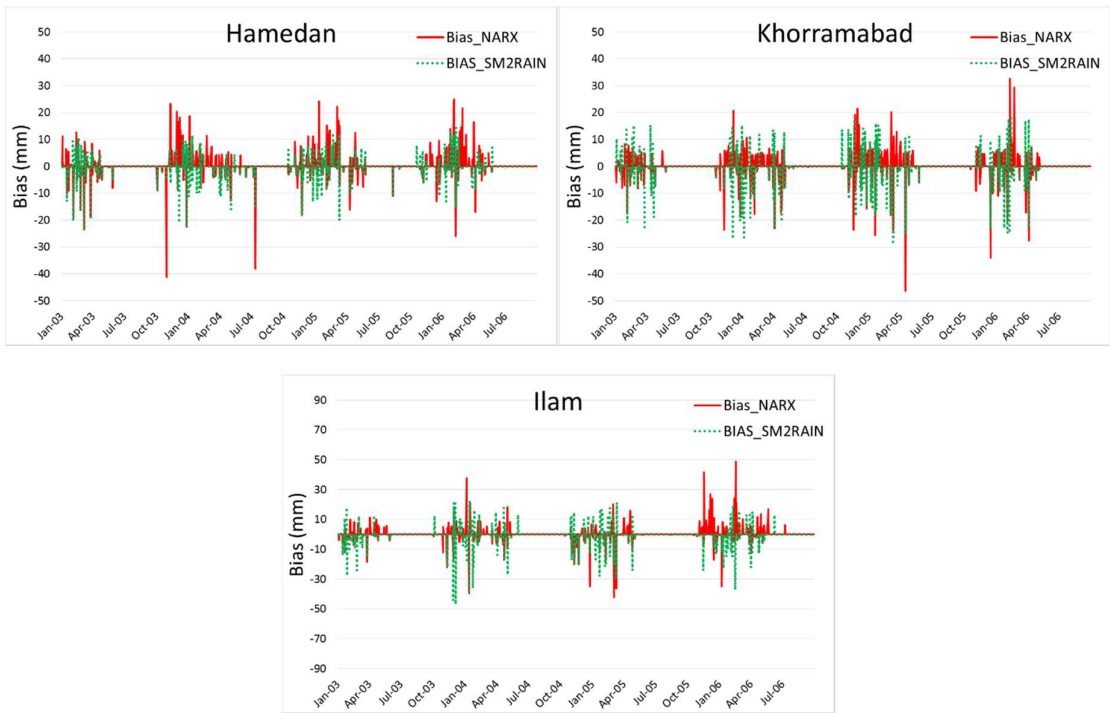


Figure 5. Bias (simulated-observed) of the NARX- and SM2RAIN- modeled rainfall for the 5 KRB stations

For station Hamedan, NARX provides almost the same, or even little better results than SM2RAIN. In contrast, for Khorramabad and Ilam stations, SM2RAIN is generally superior by delivering a higher correlation than NARX for all periods/phases. A more revealing picture of the performance-differences between the two methods is provided by the plots of the biases, i.e. the absolute differences between the simulated and observed rainfalls for the KRB stations in Figure 5. As can be clearly seen, the SM2RAIN model has for all stations generally less bias, i.e. also less RMSE (see Tables 2 and 5) than the NARX model. Moreover, as mentioned earlier, SM2RAIN has a tendency to underestimate higher rainfall rates due to saturation and this is the reason why many of the SM2RAIN- biases are negative, whereas the NARX- bias show more temporary systematic over/under prediction of the rainfall. In any case, these results indicate that a physically based model (SM2RAIN) is - at least in this application - indeed superior to a non-physical neural network model (NARX).

4. Conclusions

In this study the recently developed SM2RAIN- algorithm [26] and a new NARX- neural network model are applied to convert AMSR-E soil moisture data to predict daily rainfall at 5 climate stations in the KRB, Iran, which has been a major study region of the authors for some time. The results show that SM2RAIN is able to predict the rainfall at the KRB stations located in different climate regions - from the mountainous north to the flat south of KRB - with varying reliability. Thus, the SM2RAIN- simulated rainfall shows good correlations with the observed one, with R-values ranging from 0.44 to 0.90 during the calibration and validation period.

The new NARX neural network developed here turns out to be fast and robust and is able to also approximate the daily rainfall data at the same KRB stations in an acceptable manner, wherefore the R - values range between 0.42 and 0.76 for the testing period. From the time series of the biases obtained with the two prediction methods (Figure 5), it can be inferred that although SM2RAIN underestimates daily rainfall in many cases, this method works somewhat better than NARX which produces higher biases and RMSE (Tables 2 and 5) at all stations. Whether this holds generally, or

only in the present KRB application, is yet to be investigated. However, given that SM2RAIN is a physical model its slight superiority may be of no surprise. On the other hand, the appealing feature of the NARX network is that, thanks to the use of exogenous (external) input data, its network complexity is reduced compared with classical multilayer perceptron neural networks.

In conclusion, the results of the present study indicate that both SM2RAIN- and NARX models, using AMSR-E satellite soil moisture products, have a high potential for real-time rainfall prediction, but should be further applied with other satellite soil moisture data sets to more catchments worldwide with different physiographic characteristics, in order to better assess their practical usefulness.

Author Contributions: Majid Fereidoon completed the analysis and wrote the manuscript. Manfred Koch supervised the analysis and assisted with writing the manuscript.

Conflicts of Interest: The authors declare no conflict of interest.

References

1. Asante, K.O.; Macuacua, R.D.; Artan, G.A.; Lietzow, R.W.; Verdin, J.P. Developing a Flood Monitoring System From Remotely Sensed Data for the Limpopo Basin. *IEEE Trans. Geosci. Remote Sensing* **2007**, *45*, 1709–1714.
2. Vrochidou, A.-E.K.; Tsanis, I.K.; Grillakis, M.G.; Koutroulis, A.G. The impact of climate change on hydrometeorological droughts at a basin scale. *Journal of Hydrology* **2013**, *476*, 290–301.
3. Apurv, T.; Mehrotra, R.; Sharma, A.; Goyal, M.K.; Dutta, S. Impact of climate change on floods in the Brahmaputra basin using CMIP5 decadal predictions. *Journal of Hydrology* **2015**, *527*, 281–291.
4. Rossi, M.; Kirschbaum, D.; Valigi, D.; Mondini, A.; Guzzetti, F. Comparison of Satellite Rainfall Estimates and Rain Gauge Measurements in Italy, and Impact on Landslide Modeling. *Climate* **2017**, *5*, 90.
5. Kidd, C.; Bauer, P.; Turk, J.; Huffman, G.J.; Joyce, R.; Hsu, K.-L.; Braithwaite, D. Intercomparison of High-Resolution Precipitation Products over Northwest Europe. *J. Hydrometeor* **2012**, *13*, 67–83.
6. Rudolf, B.; Schneider, U. Calculation of gridded precipitation data for the global land-surface using in-situ gauge observations. In Proc. Second Workshop of the Int. Precipitation Working Group, Moterey, California, United States, 25-28 October 2004; pp. 231-247.
7. Yilmaz, K.K.; Hogue, T.S.; Hsu, K.-L.; Sorooshian, S.; Gupta, H.V.; Wagener, T. Intercomparison of Rain Gauge, Radar, and Satellite-Based Precipitation Estimates with Emphasis on Hydrologic Forecasting. *J. Hydrometeor* **2005**, *6*, 497–517.
8. Tian, Y.; Peters-Lidard, C.D. A global map of uncertainties in satellite-based precipitation measurements. *Geophys. Res. Lett.* **2010**, *37*, n/a-n/a.
9. Woldemeskel, F.M.; Sivakumar, B.; Sharma, A. Merging gauge and satellite rainfall with specification of associated uncertainty across Australia. *Journal of Hydrology* **2013**, *499*, 167–176.
10. Kurtzman, D.; Navon, S.; Morin, E. Improving interpolation of daily precipitation for hydrologic modelling: spatial patterns of preferred interpolators. *Hydrol. Process.* **2009**, *23*, 3281–3291.
11. Verworn, A.; Haberlandt, U. Spatial interpolation of hourly rainfall – effect of additional information, variogram inference and storm properties. *Hydrol. Earth Syst. Sci.* **2011**, *15*, 569–584.
12. Rogelis, M.C.; Werner, M.G.F. Spatial Interpolation for Real-Time Rainfall Field Estimation in Areas with Complex Topography. *J. Hydrometeor* **2013**, *14*, 85–104.
13. Stisen, S.; Tumbo, M. Interpolation of daily raingauge data for hydrological modelling in data sparse regions using pattern information from satellite data. *Hydrological Sciences Journal* **2015**, 1–16.
14. Chen, T.; Ren, L.; Yuan, F.; Yang, X.; Jiang, S.; Tang, T.; Liu, Y.; Zhao, C.; Zhang, L. Comparison of Spatial Interpolation Schemes for Rainfall Data and Application in Hydrological Modeling. *Water* **2017**, *9*, 342.

15. Zambrano-Bigiarini, M.; Nauditt, A.; Birkel, C.; Verbist, K.; Ribbe, L. Temporal and spatial evaluation of satellite-based rainfall estimates across the complex topographical and climatic gradients of Chile. *Hydrol. Earth Syst. Sci.* **2017**, *21*, 1295–1320.
16. Bowman, K.P. Comparison of TRMM Precipitation Retrievals with Rain Gauge Data from Ocean Buoys. *J. Climate* **2005**, *18*, 178–190.
17. Lo Conti, F.; Hsu, K.-I.; Noto, L.V.; Sorooshian, S. Evaluation and comparison of satellite precipitation estimates with reference to a local area in the Mediterranean Sea. *Atmospheric Research* **2014**, *138*, 189–204.
18. Stampoulis, D.; Anagnostou, E.N.; Nikolopoulos, E.I. Assessment of High-Resolution Satellite-Based Rainfall Estimates over the Mediterranean during Heavy Precipitation Events. *J. Hydrometeor* **2013**, *14*, 1500–1514.
19. Bayissa, Y.; Tadesse, T.; Demisse, G.; Shiferaw, A. Evaluation of Satellite-Based Rainfall Estimates and Application to Monitor Meteorological Drought for the Upper Blue Nile Basin, Ethiopia. *Remote Sensing* **2017**, *9*, 669.
20. Hughes, D.A. Comparison of satellite rainfall data with observations from gauging station networks. *Journal of Hydrology* **2006**, *327*, 399–410.
21. Hsu, K.-I.; Gao, X.; Sorooshian, S.; Gupta, H.V. Precipitation Estimation from Remotely Sensed Information Using Artificial Neural Networks. *J. Appl. Meteor.* **1997**, *36*, 1176–1190.
22. Sorooshian, S.; Hsu, K.-I.; Gao, X.; Gupta, H.V.; Imam, B.; Braithwaite, D. Evaluation of PERSIANN System Satellite-Based Estimates of Tropical Rainfall. *Bull. Amer. Meteor. Soc.* **2000**, *81*, 2035–2046.
23. Kidd, C.; Kniveton, D.R.; Todd, M.C.; Bellerby, T.J. Satellite Rainfall Estimation Using Combined Passive Microwave and Infrared Algorithms. *J. Hydrometeor* **2003**, *4*, 1088–1104.
24. Su, J.; Lü, H.; Wang, J.; Sadeghi, A.; Zhu, Y. Evaluating the Applicability of Four Latest Satellite–Gauge Combined Precipitation Estimates for Extreme Precipitation and Streamflow Predictions over the Upper Yellow River Basins in China. *Remote Sensing* **2017**, *9*, 1176.
25. Brocca, L.; Moramarco, T.; Melone, F.; Wagner, W. A new method for rainfall estimation through soil moisture observations. *Geophys. Res. Lett.* **2013**, *40*, 853–858.
26. Brocca, L.; Ciabatta, L.; Massari, C.; Moramarco, T.; Hahn, S.; Hasenauer, S.; Kidd, R.; Dorigo, W.; Wagner, W.; Levizzani, V. Soil as a natural rain gauge: Estimating global rainfall from satellite soil moisture data. *J. Geophys. Res. Atmos.* **2014**, *119*, 5128–5141.
27. Brocca, L.; Camici, S.; Melone, F.; Moramarco, T.; Martínez-Fernández, J.; Didon-Lescot, J.-F.; Morbidelli, R. Improving the representation of soil moisture by using a semi-analytical infiltration model. *Hydrol. Process.* **2014**, *28*, 2103–2115.
28. Ciabatta, L.; Brocca, L.; Moramarco, T.; Wagner, W. Comparison of Different Satellite Rainfall Products Over the Italian Territory. In *Engineering geology for society and territory*; Lollino, G., Arattano, M., Rinaldi, M., Giustolisi, O., Marechal, J.-C., Grant, G.E., Eds.; Springer International Publishing: Cham, Switzerland, Heidelberg [Germany], 2015, pp. 623–626.
29. Fereidoon, M.; Koch, M. SWAT-MODSIM-PSO optimization of multi-crop planning in the Karkheh River Basin, Iran, under the impacts of climate change. *Science of The Total Environment* **2018**, *630*, 502–516.
30. Ciabatta, L.; Brocca, L.; Massari, C.; Moramarco, T.; Gabellani, S.; Puca, S.; Wagner, W. Rainfall-runoff modelling by using SM2RAIN-derived and state-of-the-art satellite rainfall products over Italy. *International Journal of Applied Earth Observation and Geoinformation* **2016**, *48*, 163–173.
31. Massari, C.; Brocca, L.; Moramarco, T.; Trambly, Y.; Didon Lescot, J.-F. Potential of soil moisture observations in flood modelling: Estimating initial conditions and correcting rainfall. *Advances in Water Resources* **2014**, *74*, 44–53.

32. Wu, C.L.; Chau, K.W.; Fan, C. Prediction of rainfall time series using modular artificial neural networks coupled with data-preprocessing techniques. *Journal of Hydrology* **2010**, *389*, 146–167.
33. Philip, N.S.; Joseph, K.B. A neural network tool for analyzing trends in rainfall. *Computers & Geosciences* **2003**, *29*, 215–223.
34. Chattopadhyay, S.; Chattopadhyay, G. Comparative study among different neural net learning algorithms applied to rainfall time series. *Met. Apps* **2008**, *15*, 273–280.
35. Shukla, R.P.; Tripathi, K.C.; Pandey, A.C.; Das, I.M.L. Prediction of Indian summer monsoon rainfall using Niño indices: A neural network approach. *Atmospheric Research* **2011**, *102*, 99–109.
36. Nastos, P.T.; Moustiris, K.P.; Larissi, I.K.; Paliatatos, A.G. Rain intensity forecast using Artificial Neural Networks in Athens, Greece. *Atmospheric Research* **2013**, *119*, 153–160.
37. Abbot, J.; Marohasy, J. Input selection and optimisation for monthly rainfall forecasting in Queensland, Australia, using artificial neural networks. *Atmospheric Research* **2014**, *138*, 166–178.
38. LEONTARITIS, I.J.; BILLINGS, S.A. Input-output parametric models for non-linear systems Part I: deterministic non-linear systems. *International Journal of Control* **1985**, *41*, 303–328.
39. Lin, T.; Horne, B.G.; Tino, P.; Giles, C.L. Learning long-term dependencies in NARX recurrent neural networks. *IEEE Trans. Neural Netw.* **1996**, *7*, 1329–1338.
40. Boussaada, Z.; Curea, O.; Remaci, A.; Camblong, H.; Mrabet Bellaaj, N. A Nonlinear Autoregressive Exogenous (NARX) Neural Network Model for the Prediction of the Daily Direct Solar Radiation. *Energies* **2018**, *11*, 620.
41. Wunsch, A.; Liesch, T.; Broda, S. Forecasting groundwater levels using nonlinear autoregressive networks with exogenous input (NARX). *Journal of Hydrology* **2018**.
42. Fereidoon, M.; Koch, M.; Brocca, L. Predicting rainfall and runoff through satellite soil moisture data and SWAT modelling for a poorly gauged basin in Iran. *Journal of Hydrology* (under review).
43. Ahmad, M.-u.-D.; Giordano, M. The Karkheh River basin: the food basket of Iran under pressure. *Water International* **2010**, *35*, 522–544.
44. Tavakoli, A.R.; Oweis, T.; Ashrafi, Sh.; Asadi, H.; Siadat, H.; Liaghat, A. Improving Rainwater Productivity with Supplemental Irrigation in Upper Karkheh River Basin of Iran. International Center for Agricultural Research in the Dry Areas (ICARDA), Aleppo, Syria, 2010, 123 pp.
45. Njoku, E.G.; Jackson, T.J.; Lakshmi, V.; Chan, T.K.; Nghiem, S.V. Soil moisture retrieval from AMSR-E. *IEEE Trans. Geosci. Remote Sensing* **2003**, *41*, 215–229.
46. Jackson, T.J.; Cosh, M.H.; Bindlish, R.; Starks, P.J.; Bosch, D.D.; Seyfried, M.; Goodrich, D.C.; Moran, M.S.; Du, J. Validation of Advanced Microwave Scanning Radiometer Soil Moisture Products. *IEEE Trans. Geosci. Remote Sensing* **2010**, *48*, 4256–4272.
47. Brocca, L.; Massari, C.; Ciabatta, L.; Moramarco, T.; Penna, D.; Zuecco, G.; Pianezzola, L.; Borga, M.; Matgen, P.; Martínez-Fernández, J. Rainfall estimation from in situ soil moisture observations at several sites in Europe: an evaluation of the SM2RAIN algorithm. *Journal of Hydrology and Hydromechanics* **2015**, *63*, 13.
48. Famiglietti, J.S.; Wood, E.F. Multiscale modeling of spatially variable water and energy balance processes. *Water Resour. Res.* **1994**, *30*, 3061–3078.
49. Doorenbos, J.; Pruitt, W.O. Background and Development of Methods to Predict Reference Crop Evapotranspiration (ET_o). Appendix II in FAO-ID-24, 1977, pp. 108–119.
50. Zare, M.; Koch, M. Using ANN and ANFIS Models for simulating and predicting Groundwater Level Fluctuations in the Miandarband Plain, Iran. Proceedings of the 4th IAHR Europe Congress. Sustainable Hydraulics in the Era of Global Change, Liege, Belgium, 27-29 July 2016; p. 416.

420 51. Ince, H. Non-Parametric Regression Methods. *CMS* **2006**, *3*, 161–174.
421 52. Bishop, C.M. *Neural networks for pattern recognition*; Clarendon Press: Oxford, 1995.
422 53. Terzic, E.; Nagarajah, C.R.; Alamgir, M. Capacitive sensor-based fluid level measurement in a dynamic environment
423 using neural network. *Engineering Applications of Artificial Intelligence* **2010**, *23*, 614–619.
424 54. Hung, N.Q.; Babel, M.S.; Weesakul, S.; Tripathi, N.K. An artificial neural network model for rainfall forecasting in
425 Bangkok, Thailand. *Hydrol. Earth Syst. Sci.* **2009**, *13*, 1413–1425.
426 55. Pearlmutter, B. Dynamic recurrent neural networks. Technical report CMU-CS-90-196, School of Computer Science,
427 Carnegie Mellon University, Pittsburgh, Pennsylvania, USA, 1990.
428 56. Ćirović, V.; Aleksendrić, D.; Mladenović, D. Braking torque control using recurrent neural networks. *Proceedings of*
429 *the Institution of Mechanical Engineers, Part D: Journal of Automobile Engineering* **2012**, *226*, 754–766.
430 57. Huo, F.; Poo, A.-N. Nonlinear autoregressive network with exogenous inputs based contour error reduction in CNC
431 machines. *International Journal of Machine Tools and Manufacture* **2013**, *67*, 45–52.
432 58. Beale, M.H.; Hagan, M.T.; Demuth, H.B. Neural network toolbox™ user’s guide. In R2012a. The MathWorks, Inc., 3
433 Apple Hill Drive Natick, MA 01760-2098, www.mathworks.com.
434 59. Crow, W.T.; Berg, A.A.; Cosh, M.H.; Loew, A.; Mohanty, B.P.; Panciera, R.; Rosnay, P. de; Ryu, D.; Walker, J.P.
435 Upscaling sparse ground-based soil moisture observations for the validation of coarse-resolution satellite soil moisture
436 products. *Rev. Geophys.* **2012**, *50*, 3675.
437 60. Chen, F.; Crow, W.T.; Ryu, D. Dual Forcing and State Correction via Soil Moisture Assimilation for Improved
438 Rainfall–Runoff Modeling. *J. Hydrometeor* **2014**, *15*, 1832–1848.
439

442
443
444
445